

RECOMMENDATION ITU-R P.681-3*

**PROPAGATION DATA REQUIRED FOR THE DESIGN OF EARTH-SPACE
LAND MOBILE TELECOMMUNICATION SYSTEMS**

(Question ITU-R 207/3)

(1990-1994-1995-1997)

The ITU Radiocommunication Assembly,

considering

- a) that for the proper planning of Earth-space land mobile systems it is necessary to have appropriate propagation data and prediction methods;
- b) that the methods of Recommendation ITU-R P.618 are recommended for the planning of Earth-space telecommunication systems;
- c) that further development of prediction methods for specific application to land mobile-satellite systems is required to give adequate accuracy in all regions of the world and for all operational conditions;
- d) that, however, methods are available which yield sufficient accuracy for many applications,

recommends

1 that the methods contained in Annex 1 be adopted for use in the planning of Earth-space land mobile telecommunications systems, in addition to the methods recommended in Recommendation ITU-R P.618.

ANNEX 1

1 Introduction

Propagation effects in the land mobile-satellite service (LMSS) differ from those of the fixed-satellite service (FSS) primarily because of the greater importance of terrain effects. In the FSS it is generally possible to discriminate against multipath, shadowing and blockage through the use of highly directive antennas placed at unobstructed sites. Therefore, in general, the LMSS offers smaller link availability percentages than the FSS. The prime availability range of interest to system designers is usually from 80% to 99%.

This Annex deals with data and models specifically needed for predicting propagation impairments in LMSS links, which include tropospheric effects, ionospheric effects, multipath, blockage and shadowing. It is based on measurements at 1.5 GHz (L-band) and 870 MHz in the UHF band.

2 Tropospheric effects**2.1 Attenuation**

Signal losses in the troposphere are caused by atmospheric gases, rain, fog and clouds. Except at low elevation angles, tropospheric attenuation is negligible at frequencies below about 1 GHz, and is generally small at frequencies up to about 10 GHz. Above 10 GHz, the attenuation can be large for significant percentages of the time on many paths.

* This Recommendation should be brought to the attention of Radiocommunication Study Group 8.

Prediction methods are available for estimating gaseous absorption (Recommendation ITU-R P.676) and rain attenuation (Recommendation ITU-R P.618). Fog and cloud attenuation is usually negligible for frequencies up to 10 GHz.

2.2 Scintillation

Irregular variations in received signal level and in angle of arrival are caused by both tropospheric turbulence and atmospheric multipath. The magnitudes of these effects increase with increasing frequency and decreasing path elevation angle, except that angle-of-arrival fluctuations caused by turbulence are independent of frequency. Antenna beamwidth also affects the magnitude of these scintillations. These effects are observed to be at a maximum in the summer season. A prediction method is given in Recommendation ITU-R P.618.

3 Ionospheric effects

Ionospheric effects on Earth-to-space paths are addressed in Recommendation ITU-R P.531. Values of ionospheric effects for frequencies in the range of 0.1 to 10 GHz are given in Tables 1 and 2 of Recommendation ITU-R P.680.

4 Shadowing

Cumulative fade distribution measurements at 870 MHz, 1.6 GHz and 20 GHz have been used to develop the extended empirical roadside shadowing model (EERS). The extent of trees along the roadside is represented by the percentage of optical shadowing caused by roadside trees at a path elevation angle of 45° in the direction of the signal source. The model is valid when this percentage is in the range 55-75%.

4.1 Calculation of fading due to shadowing by roadside trees

The following procedure provides estimates of roadside shadowing for frequencies between 800 MHz and 20 GHz, path elevation angles from 7° up to 60°, and percentages of distance travelled from 1% to 80%. The empirical model corresponds to an average propagation condition with the vehicle driving in lanes on both sides of the roadway (lanes close to and far from the roadside trees are included). The predicted fade distributions apply for highways and rural roads where the overall aspect of the propagation path is, for the most part, orthogonal to the lines of roadside trees and utility poles and it is assumed that the dominant cause of LMSS signal fading is tree canopy shadowing (see Recommendation ITU-R P.833).

Parameters required are the following:

f : frequency (GHz)

θ : path elevation angle to the satellite (degrees)

p : percentage of distance travelled over which fade is exceeded.

Step 1: Calculate the fade distribution at 1.5 GHz, valid for percentages of distance travelled of $20\% \geq p \geq 1\%$, at the desired path elevation angle, $60^\circ \geq \theta \geq 20^\circ$:

$$A_L(p, \theta) = -M(\theta) \ln(p) + N(\theta) \quad (1)$$

where:

$$M(\theta) = 3.44 + 0.0975 \theta - 0.002 \theta^2 \quad (2)$$

$$N(\theta) = -0.443 \theta + 34.76 \quad (3)$$

Step 2: Convert the fade distribution at 1.5 GHz, valid for $20\% \geq p \geq 1\%$, to the desired frequency, f (GHz), where $0.8 \text{ GHz} \leq f \leq 20 \text{ GHz}$:

$$A_{20}(p, \theta, f) = A_L(p, \theta) \exp \left\{ 1.5 \left[\frac{1}{\sqrt{f_{1.5}}} - \frac{1}{\sqrt{f}} \right] \right\} \quad (4)$$

Step 3: Calculate the fade distribution for percentages of distance travelled $80\% \geq p > 20\%$ for the frequency range $0.85 \text{ GHz} \leq f \leq 20 \text{ GHz}$ as:

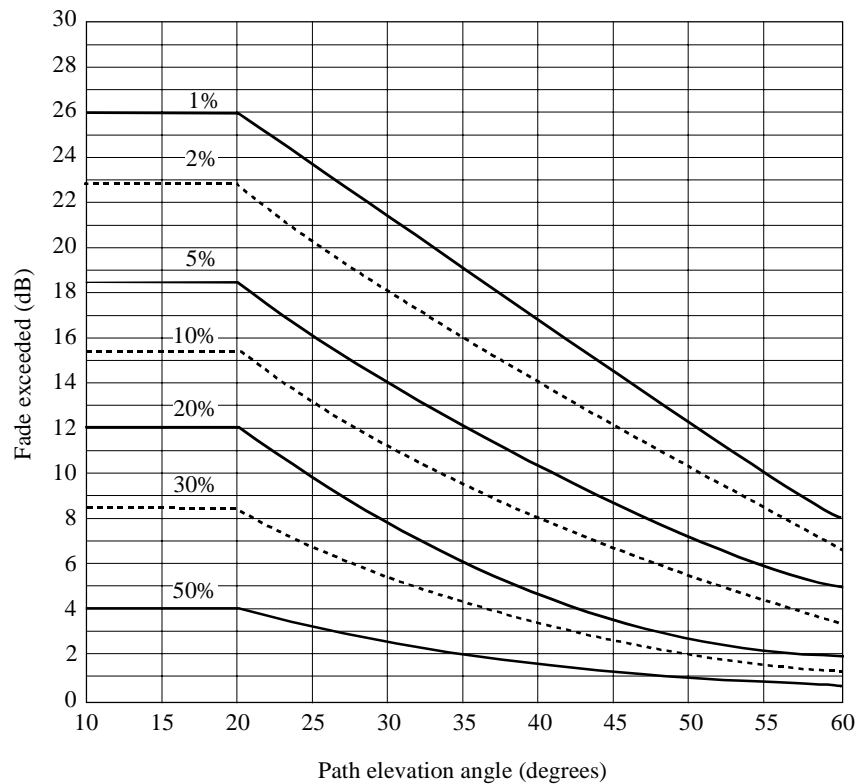
$$A(p, \theta, f) = A_{20}(20\%, \theta, f) \frac{1}{\ln 4} \ln \left(\frac{80}{p} \right) \quad \text{for} \quad 80\% \geq p > 20\% \quad (5)$$

$$= A_{20}(p, \theta, f) \quad \text{for} \quad 20\% \geq p > 1\%$$

Step 4: For path elevation angles in the range $20^\circ > \theta \geq 7^\circ$, the fade distribution is assumed to have the same value as at $\theta = 20^\circ$.

Figure 1 shows fades exceeded at 1.5 GHz versus elevation angles between 10° and 60° for a family of equal percentages between 1% and 50%.

FIGURE 1
Fading at 1.5 GHz due to roadside shadowing versus path elevation angle



0681-01

4.1.1 Extension to elevation angles > 60°

The roadside shadowing model at frequencies of 1.6 GHz and 2.6 GHz can be extended to elevation angles above 60° with the following procedure:

- apply equations (1) to (5) at an elevation angle of 60° at the above frequencies;
- linearly interpolate between the value calculated for an angle of 60° and the fade values for an elevation angle of 80° provided in Table 1;
- linearly interpolate between the values in Table 1 and a value of zero at 90°.

TABLE 1

Fades exceeded (dB) at 80° elevation

P (%)	Tree-shadowed	
	1.6 GHz	2.6 GHz
1	4.1	9.0
5	2.0	5.2
10	1.5	3.8
15	1.4	3.2
20	1.3	2.8
30	1.2	2.5

4.1.2 Application of roadside shadowing model to non-GSO land mobile-satellite systems

The prediction method above was derived for, and is applied to, LMSS geometries where the elevation angle remains constant. For non-GSO systems, where the elevation angle is varying, the link availability can be calculated in the following way:

- calculate the percentage of time for each elevation angle (or elevation angle range) under which the terminal will see the spacecraft;
- for a given propagation margin (ordinate of Fig. 1), find the percentage of unavailability for each elevation angle;
- for each elevation angle, multiply the results of a) and b) and divide by 100, giving the percentage of unavailability of the system at this elevation;
- add up all unavailability values obtained in c) to arrive at the total system unavailability.

If the antenna used at the mobile terminal does not have an isotropic pattern, the antenna gain at each elevation angle has to be subtracted from the fade margin in step b) above.

In the case of multi-visibility satellite constellations employing satellite path diversity (i.e. switching to the least impaired path), an approximate calculation can be made assuming that the spacecraft with the highest elevation angle is being used.

4.2 Fade duration distribution model

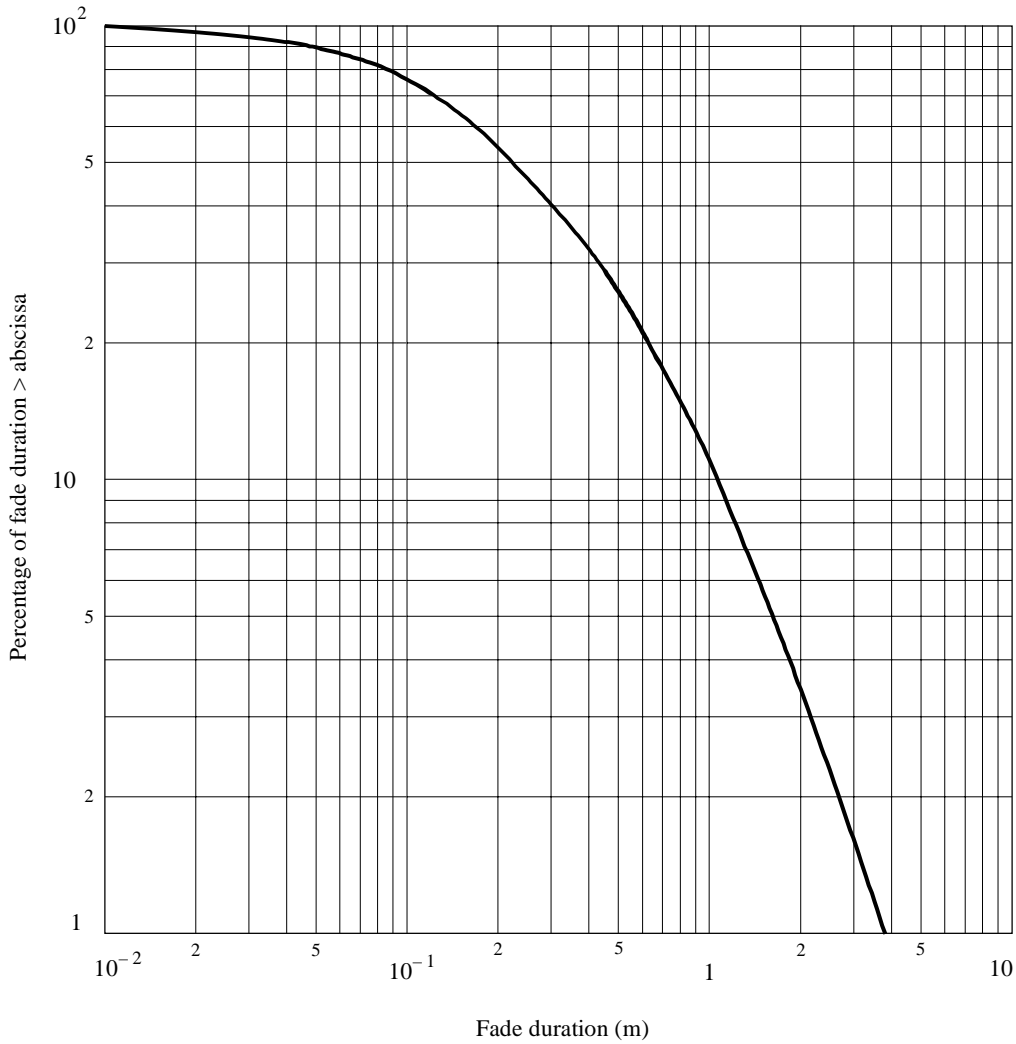
Optimal design of land mobile satellite receivers depends on knowledge of the statistics associated with fade durations, which can be represented in units of travelled distance (m) or (s). Fade duration measurements have given rise to the following empirical model which is valid for distance fade duration $dd \geq 0.02$ m.

$$P(FD > dd \mid A > A_q) = \frac{1}{2} \left(1 - \operatorname{erf} \left[\frac{\ln(dd) - \ln(\alpha)}{\sqrt{2} \sigma} \right] \right) \quad (6)$$

where $P(FD > dd \mid A > A_q)$ represents the probability that the distance fade duration, FD , exceeds the distance, dd (m), under the condition that the attenuation, A , exceeds A_q . The designation “erf” represents the error function, σ is the standard deviation of $\ln(dd)$, and $\ln(\alpha)$ is the mean value of $\ln(dd)$. The left-hand side of equation (6) was estimated by computing the percentage number of “duration events” that exceed dd relative to the total number of events for which $A > A_q$ in data obtained from measurements in the United States of America and Australia. The best fit regression values obtained from these measurements are $\alpha = 0.22$ and $\sigma = 1.215$.

Figure 2 contains a plot of P , expressed as a percentage, p , versus dd for a 5 dB threshold.

FIGURE 2
Best fit cumulative fade distribution for roadside tree shadowing with a 5 dB threshold



0681-02

The model given by equation (6) is based on measurements at an elevation angle of 51° and is applicable for moderate to severe shadowing (percentage of optical shadowing 55%-90%). Tests at 30° and 60° have demonstrated a moderate dependence on elevation angle: the smaller the elevation angle, the larger is the fade duration for a fixed percentage. For example, the 30° fade duration showed approximately twice that for the 60° fade duration at the same percentage level.

4.3 Non-fade duration distribution model

A “non-fade duration” event of distance duration, dd , is defined as the distance over which the fade levels are smaller than a specified fade threshold. The non-fade duration model is given by:

$$P(NFD > dd \mid A < A_q) = \beta (dd)^{-\gamma} \tag{7}$$

where $P(NFD > dd \mid A < A_q)$ is the percentage probability that a continuous non-fade distance, NFD , exceeds the distance, dd , given that the fade is smaller than the threshold, A_q . Table 2 contains the values of β and γ for roads that exhibit “moderate and extreme” shadowing i.e. the percentage of optical shadowing of 55%-75% and 75%-90% respectively. A 5 dB fade threshold is used for A_q .

TABLE 2

Non-fade duration regression values for a 5 dB fade threshold at a path elevation angle of 51°

Shadowing level	β	γ
Moderate	20.54	0.58
Extreme	11.71	0.8371

4.4 Special consideration of handheld terminals (user blockage)

When using handheld communication terminals, the operator's head or body in the near-field of the antenna causes the antenna pattern to change. For the case of non-LEO satellite systems (GSO, HEO, ICO), the user of the handheld terminal is expected to be cooperative, i.e. to position himself in such a way as to avoid blockage from both the head (or body) and the environment. For LEO systems this assumption cannot be made. The influence of the head (or body) can be evaluated by including the modified antenna pattern (which has to be measured) in the link availability calculation as presented in § 4.1.2. Assuming that the azimuth angles under which the satellite is seen are evenly distributed, an azimuth-averaged elevation pattern can be applied. The small movements of the head or hand which lead to small variations in apparent elevation angle can also be averaged.

Relating to this effect, a field experiment was performed in Japan. Figure 3a shows the geometry of a human head and an antenna in the experiment. The satellite elevation angle is 32° and the satellite signal frequency is 1.5 GHz. The antenna gain is 1 dBi and the length is 10 cm. Figure 3b shows the variation of relative signal level versus azimuth angle ϕ in Fig. 3a. It can be seen from Fig. 3b that the maximum reduction in signal level due to user blockage is about 6 dB when the equipment is in the shadow region of the human head.

The results presented in Fig. 3b are intended to be illustrative only, since the data correspond to a single elevation angle and antenna pattern, and no account is taken of potential specular reflection effects, which may play a significant role in a handheld environment where little directivity is provided.

5 Multipath models for clear line-of-sight conditions

In many cases the mobile terminal has a clear line-of-sight (negligible shadowing) to the mobile satellite. Degradation to the signal can still occur under these circumstances, due to terrain-induced multipath. The mobile terminal receives a phasor summation of the direct line-of-sight signal and several multipath signals. These multipath signals may add constructively or destructively to result in signal enhancement or fade. The multipath signal characteristics depend on the scattering cross-sections of the multipath reflectors, their number, the distances to the receiving antenna, the field polarizations, and receiving antenna gain pattern.

The multipath degradation models introduced in the following sections are based on measurements made using an antenna with the following characteristics:

- omnidirectional in azimuth;
- gain variation between 15° and 75° elevation less than 3 dB;
- below the horizon (negative elevation angles) the antenna gain was reduced by at least 10 dB.

FIGURE 3a
Geometry of a human head and an antenna

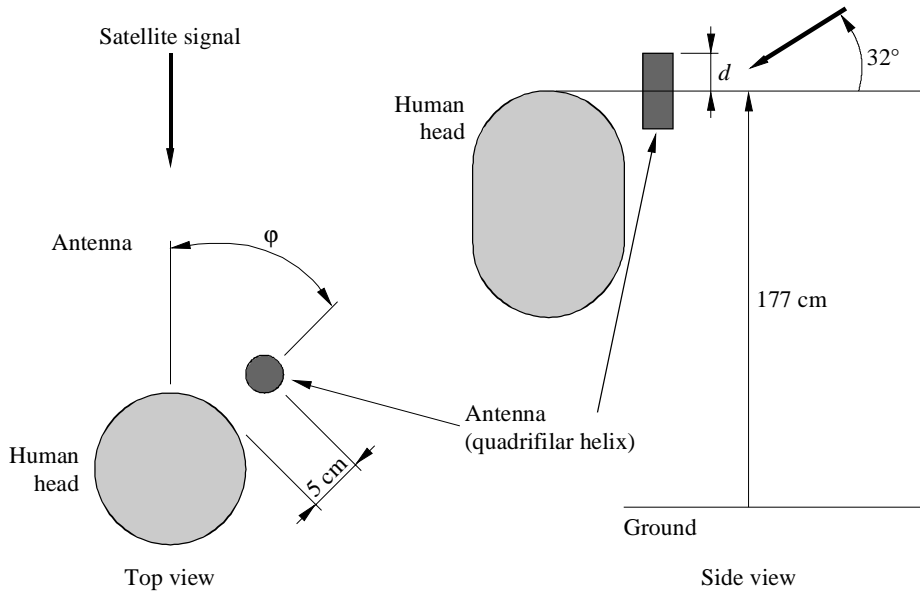
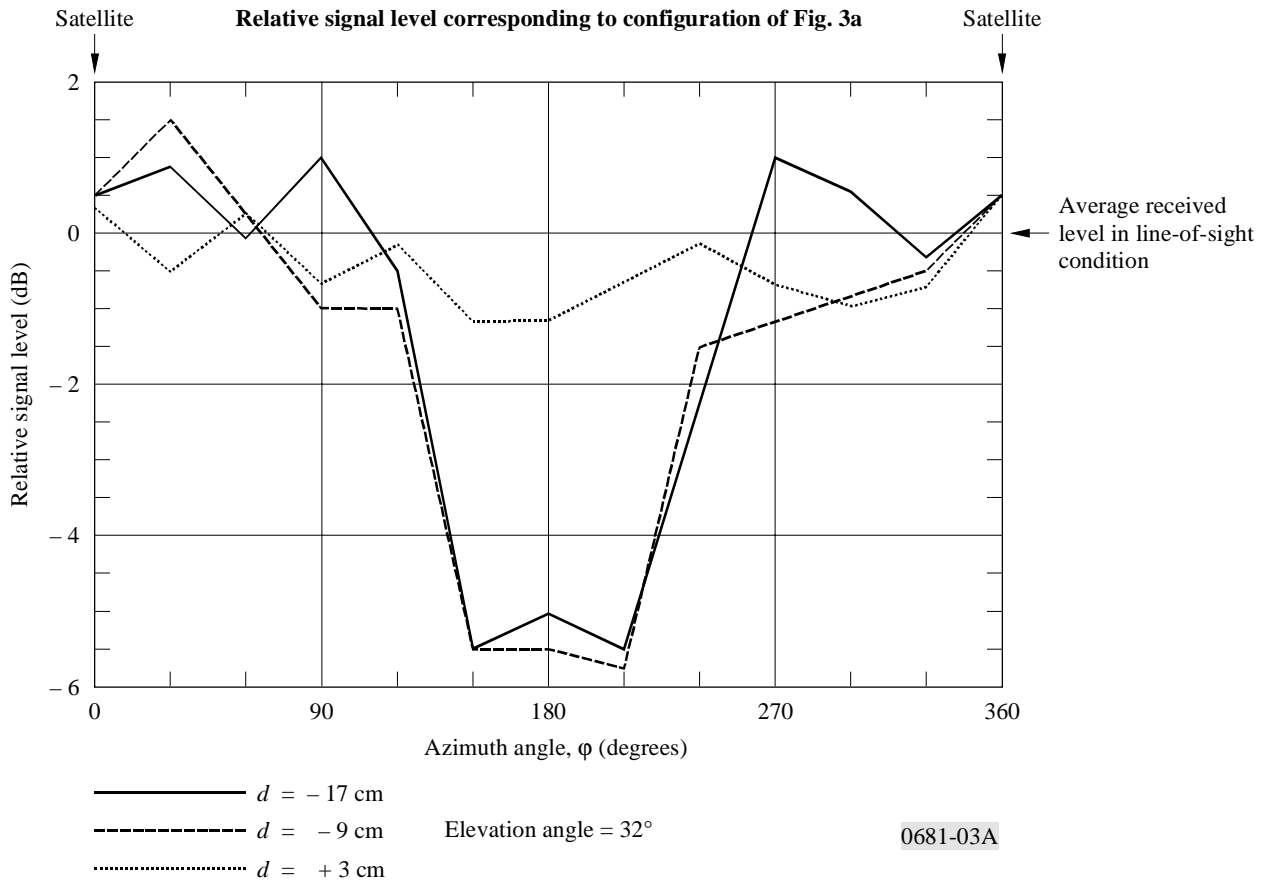


FIGURE 3b



5.1 Multipath in a mountain environment

The distribution of fade depths due to multipath in mountainous terrain is modelled by:

$$p = a A^{-b} \quad (8)$$

for:

$$1\% < p < 10\%$$

where:

p : percentage of distance over which the fade is exceeded

A : fade exceeded (dB).

The curve fit parameters, a and b , are shown in Table 3 for 1.5 GHz and 870 MHz. Note that the above model is valid when the effect of shadowing is negligible.

TABLE 3

Parameters for best fit cumulative fade distribution for multipath in mountainous terrain

Frequency (GHz)	Elevation = 30°			Elevation = 45°		
	a	b	Range (dB)	a	b	Range (dB)
0.87	34.52	1.855	2-7	31.64	2.464	2-4
1.5	33.19	1.710	2-8	39.95	2.321	2-5

Figure 4 contains curves of the cumulative fade distributions for path elevation angles of 30° and 45° at 1.5 GHz and 870 Hz.

5.2 Multipath in a roadside tree environment

Experiments conducted along tree-lined roads in the United States of America have shown that multipath fading is relatively insensitive to path elevation over the range of 30°-60°. The measured data have given rise to the following model:

$$p = u \exp(-vA) \quad (9)$$

for:

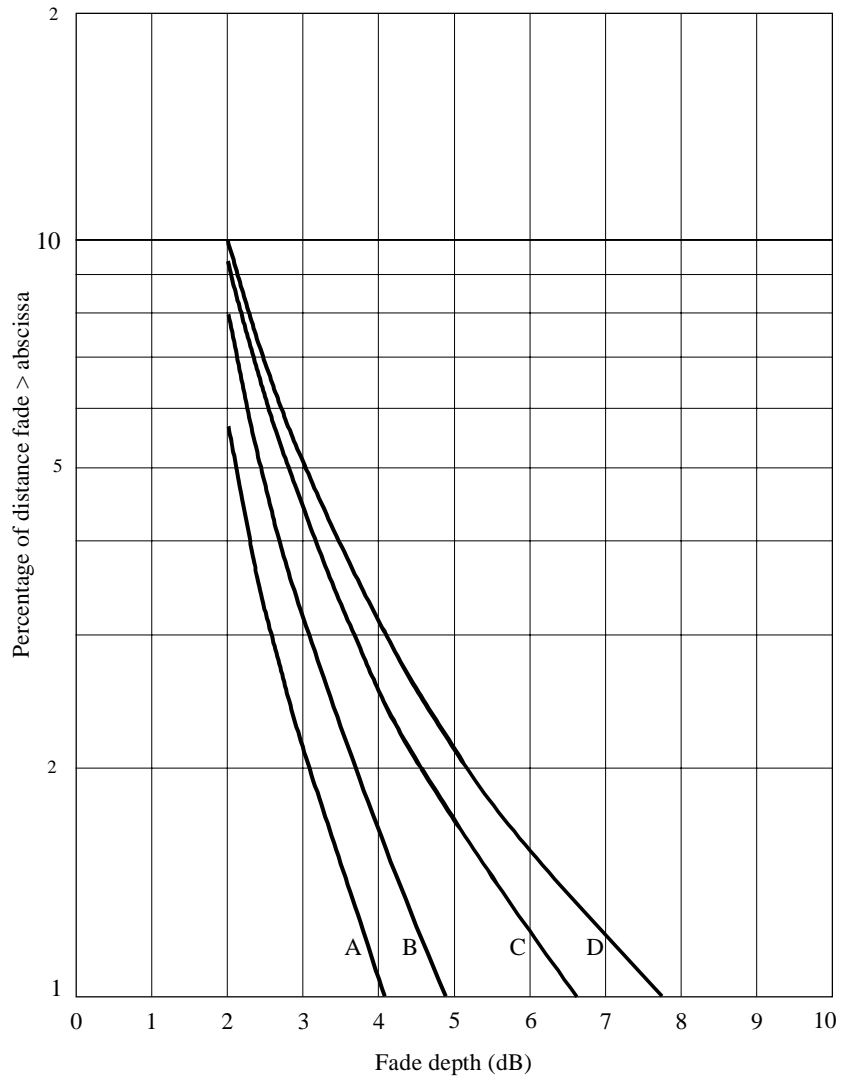
$$1\% < p < 50\%$$

where:

p : percentage of distance over which the fade is exceeded

A : fade exceeded (dB).

FIGURE 4
Best fit cumulative fade distributions for multipath fading in mountainous terrain



Curves A: 870 MHz, 45°
 B: 1.5 GHz, 45°
 C: 870 MHz, 30°
 D: 1.5 GHz, 30°

0681-04

Note that the above model assumes negligible shadowing. The curve fit parameters, u and v , are shown in Table 4.

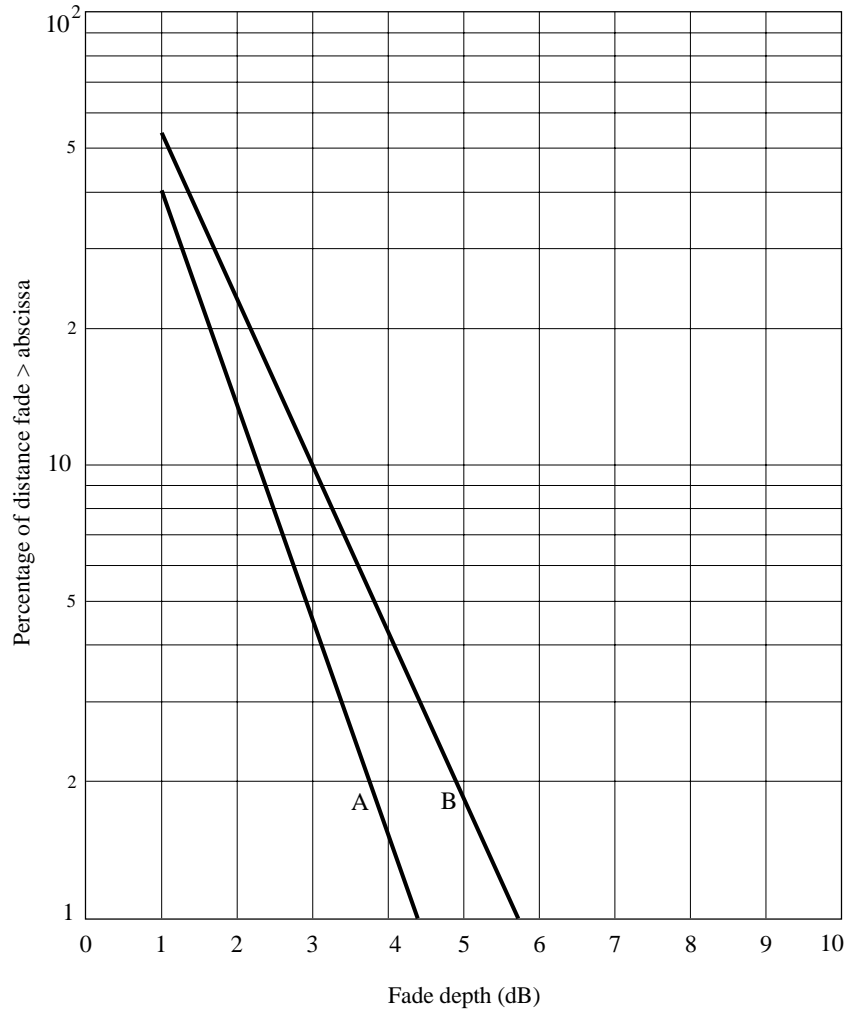
TABLE 4
Parameters for best exponential fit cumulative fade distributions for multipath for tree-lined roads

Frequency (GHz)	u	v	Fade range (dB)
0.870	125.6	1.116	1-4.5
1.5	127.7	0.8573	1-6

Figure 5 contains curves of the cumulative fade distributions for 1.5 GHz and 870 MHz. Enhanced fading due to multipath can occur at lower elevation angles (5° to 30°) where forward scattering from relatively smooth rolling terrain can be received from larger distances.

FIGURE 5

Best fit cumulative fade distributions for multipath fading on tree-lined roads



Curves A: 870 MHz

B: 1.5 GHz

0681-05

